Photocurrent-generating properties of bulk and few-layered Cd(II) coordination polymers based on a rigid dicarboxylate ligand

Peng Gang Jiang,[a] Pan Zhang,[a] Yun Gong [*a] and Jian Hua Lin[*a, b]

[a] *Department of Applied Chemistry, College of Chemistry and Chemical Engineering, Chongqing University, Chongqing 400030, P. R. China Tel: +86-023-65106150 E-mail:gongyun7211@cqu.edu.cn*

[b] *State Key Laboratory of Rare Earth Materials Chemistry and Applications, College of Chemistry and Molecular Engineering, Peking University, Beijing 100871, P. R. China Tel: +86-010-62753541 E-mail: jhlin@pku.edu.cn*

Table S1 Selected bond lengths (Å) and angles (º) for CPs **1** and **2**

CP 1			
Cd(1)-O(5)	2.114(9)	Cd(1)-O(1)	2.304(9)
Cd(1)-O(3)#1	2.206(12)	Cd(2)-O(4)#1	2.200(10)
Cd(2)-O(2)	2.379(9)	Cd(2)-O(7)	2.301(13)
Cd(2)-O(8)	2.375(17)	Cd(2)-O(1)	2.358(8)
O(5)#2-Cd(1)-O(5)	180.0(7)	O(5)#2-Cd(1)-O(1)	86.2(4)
O(5)-Cd(1)-O(3)#1	92.2(4)	O(3)#1-Cd(1)-O(1)	87.7(4)
O(6)-Cd(2)-O(8)	167.7(5)	O(1)-Cd(2)-O(2)	54.9(3)
O(6)-Cd(2)-O(1)	97.3(3)	O(7)-Cd(2)-O(8)	83.4(7)
O(4)#1-Cd(2)-O(2)	156.6(4)	O(4)#1-Cd(2)-O(1)	105.3(3)
CP 2			
Cd(1)-O(5)	2.244(9)	Cd(1)-O(2)	2.286(9)

Cd(1)-O(3)#2	2.546(9)	Cd(1)-O(1)	2.496(9)
Cd(1)-O(4)#2	2.304(9)	Cd(1)-O(3)#3	2.391(9)
O(2)-Cd(1)-O(1)	54.3(3)	O(1)-Cd(1)-O(3)#2	176.7(3)
O(5)-Cd(1)-O(2)	137.8(4)	O(4)#2-Cd(1)-O(3)#3	85.7(3)
O(4)#2-Cd(1)-O(1)	129.6(3)	O(2)-Cd(1)-O(3)#3	104.7(3)

Symmetry transformations used to generate equivalent atoms:

#1 x-1/2, -y-1/2, z-1/2 #2 -x+1, -y, -z #3 -x+1/2, -y, z+1/2

(**a**)

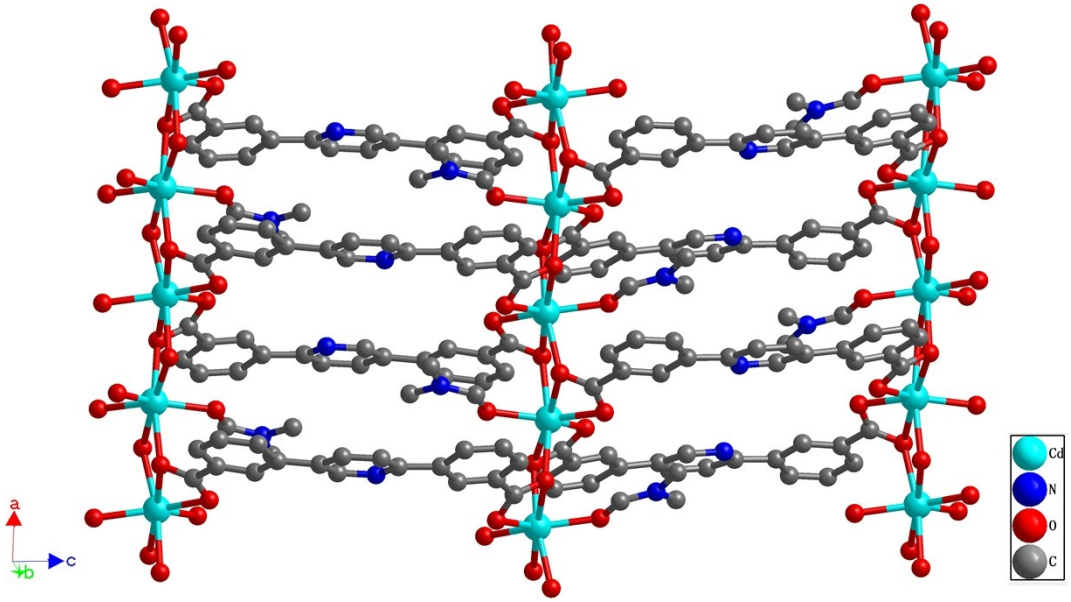

(**b**)

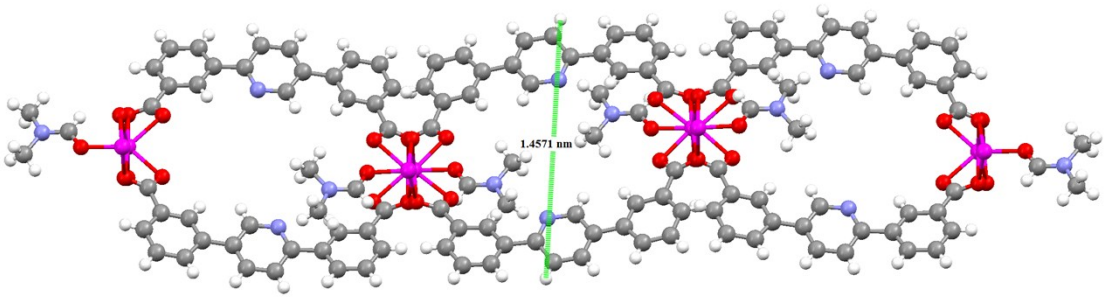

(**c**)

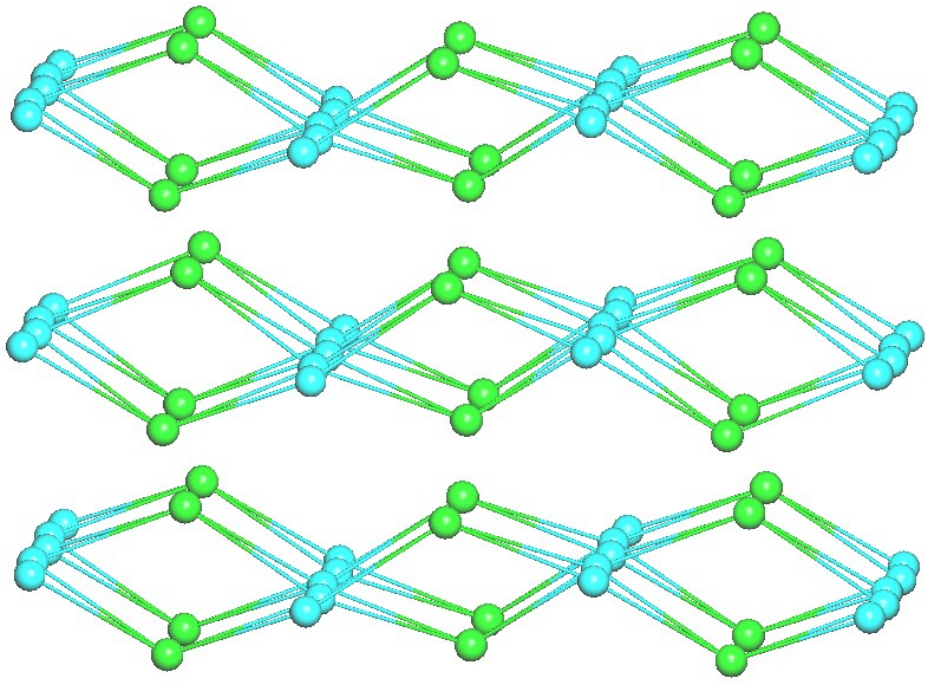

Fig. S1 2D architecture constructed by Cd(II) ions and $\mathbf{L}^{2-}$ ligands (H atoms and uncoordinated DMF molecules omitted for clarity) (**a, b**); Schematic illustrating the stacking mode of different 2D layers in CP **2** (sapphire nodes, Cd(II); green, tetradentate $\mathbf{L}^{2-}$) (**c**).

(**a**)

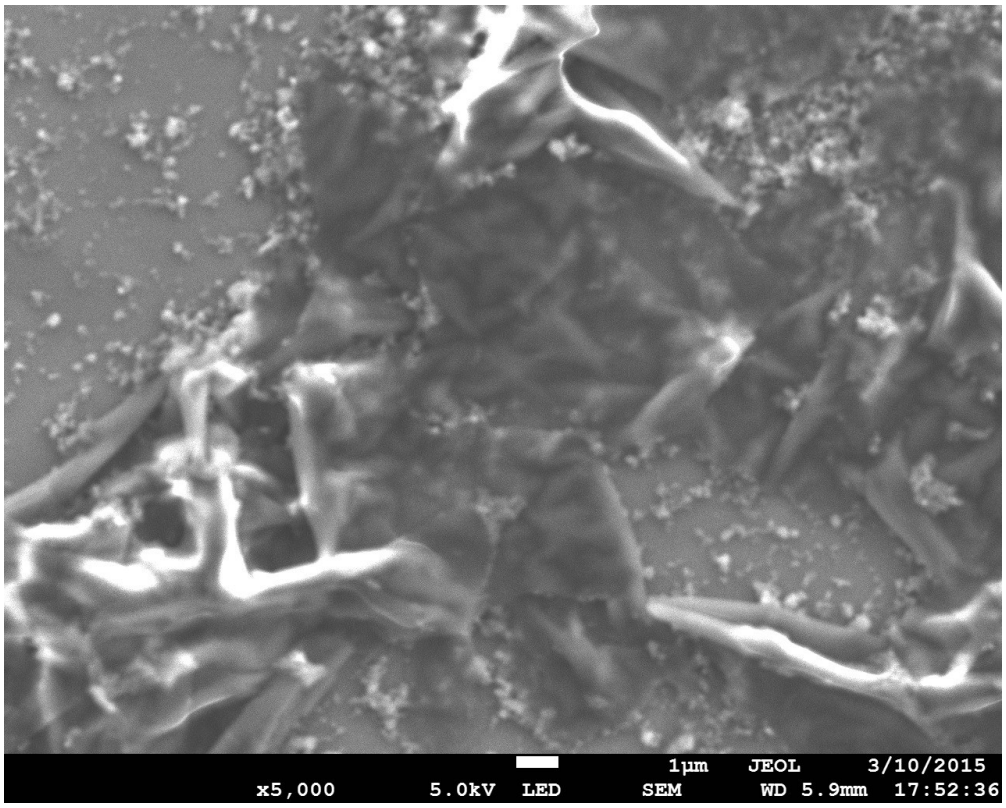
1µm JEOL 3/10/2015
x5,000 5.0kV LED SEM WD 5.9mm 17:52:36

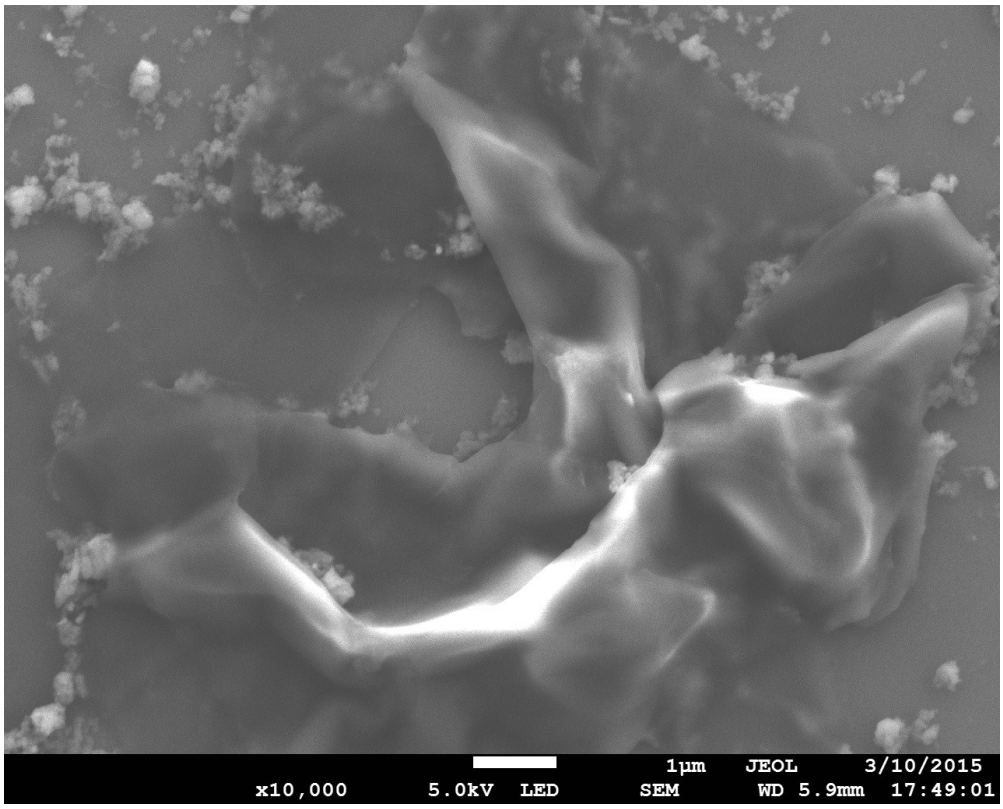
1µm JEOL 3/10/2015
x10,000 5.0kV LED SEM WD 5.9mm 17:49:01

(**b**)

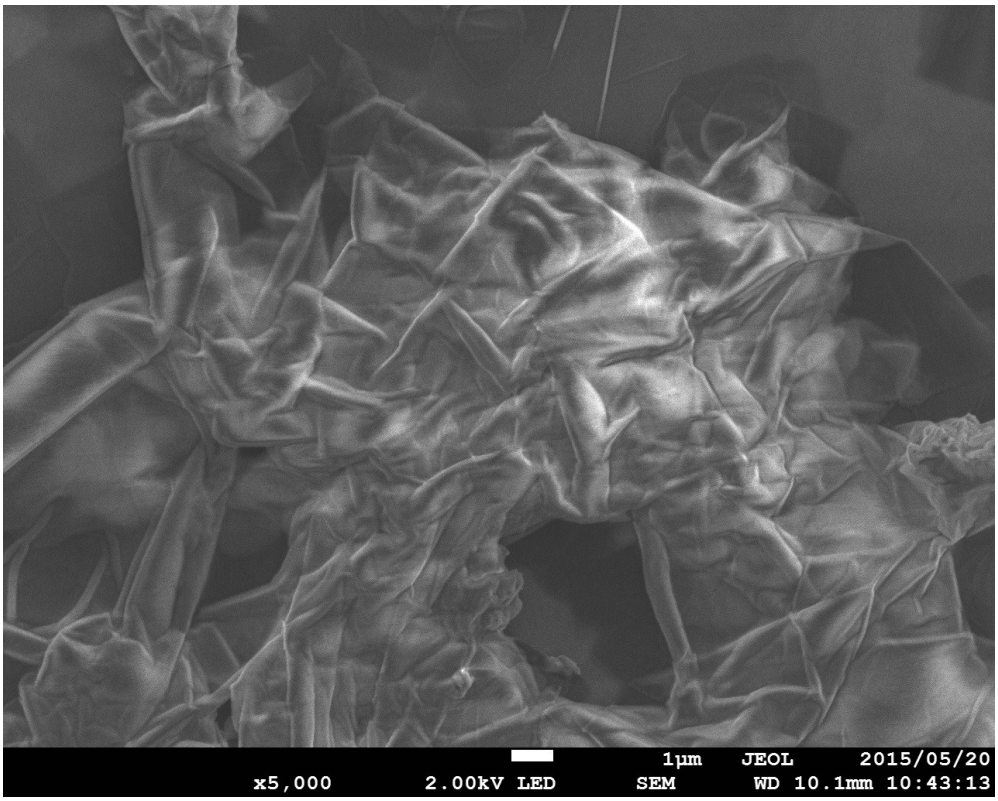
1µm JEOL 2015/05/20
x5,000 2.00kV LED SEM WD 10.1mm 10:43:13

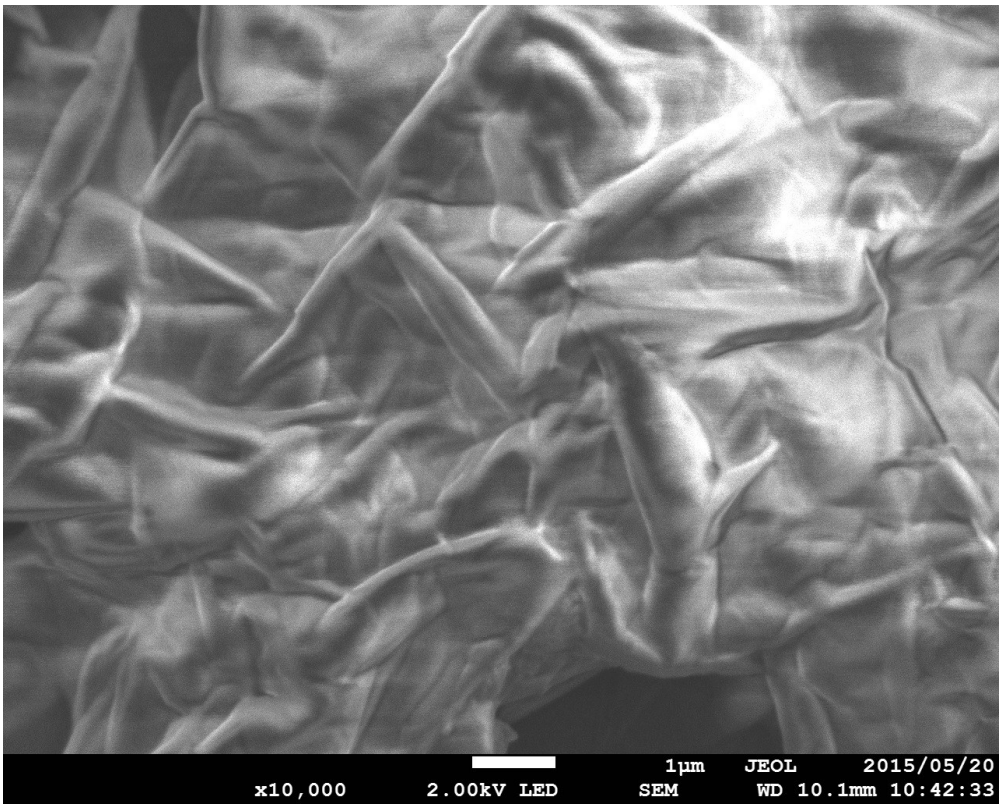
1µm JEOL 2015/05/20
x10,000 2.00kV LED SEM WD 10.1mm 10:42:33

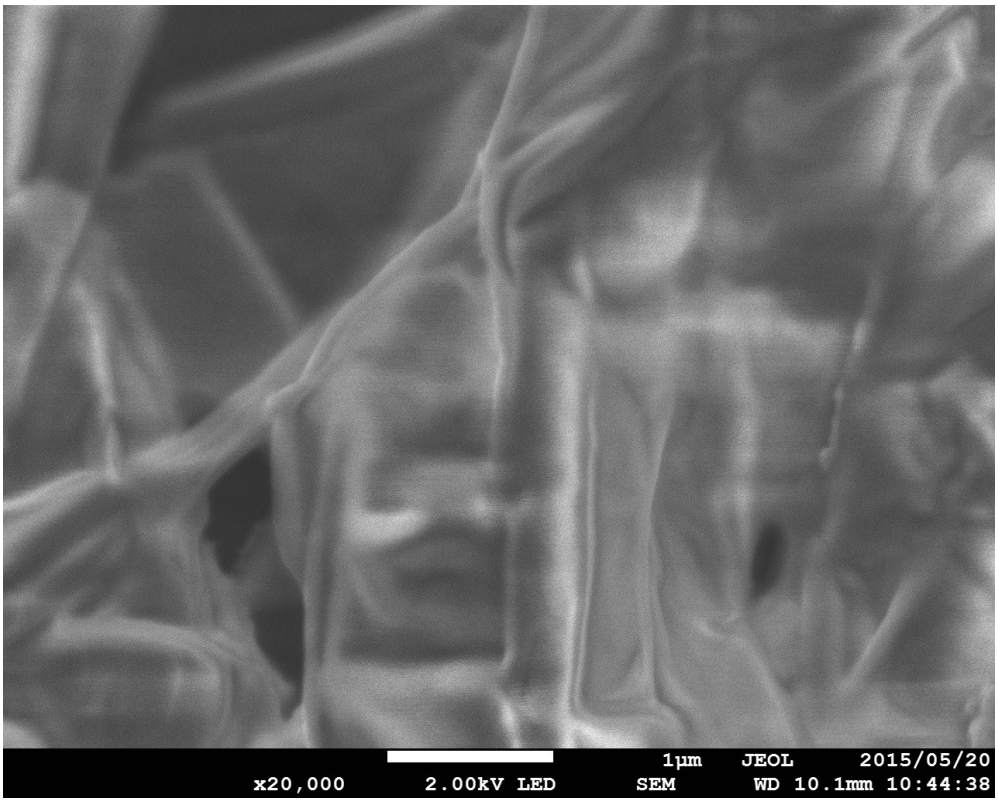
1µm JEOL 2015/05/20
x20,000 2.00kV LED SEM WD 10.1mm 10:44:38

(**c**)

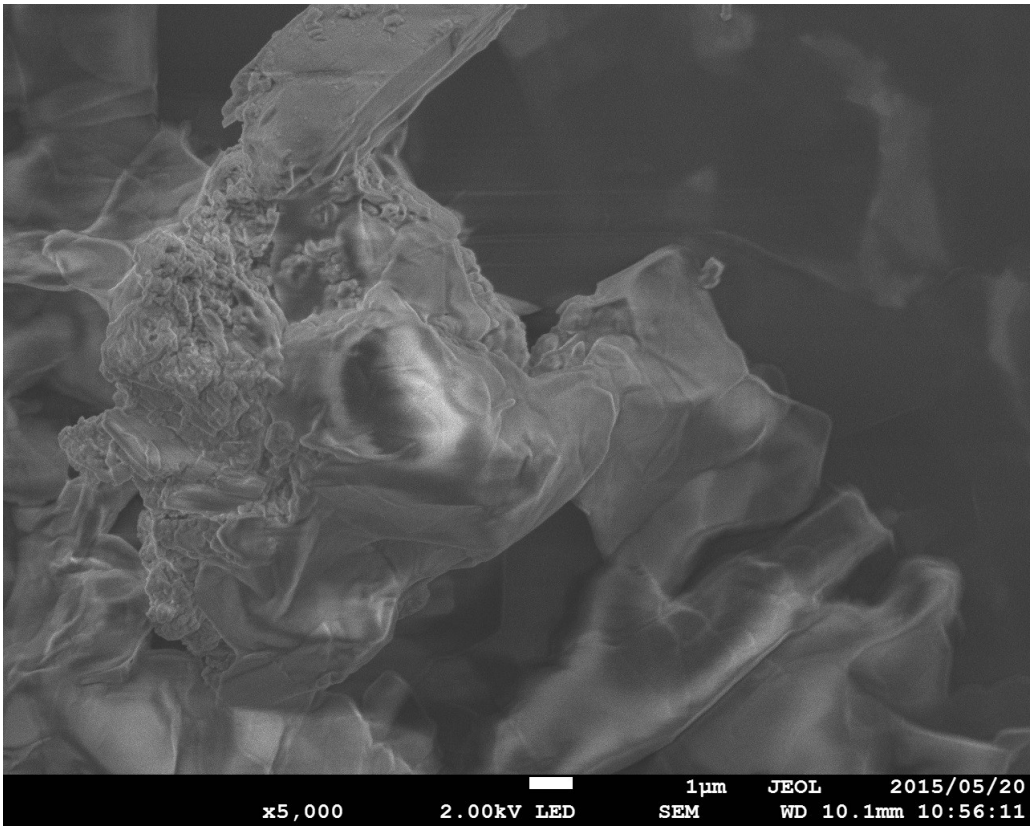
1µm JEOL 2015/05/20
x5,000 2.00kV LED SEM WD 10.1mm 10:56:11

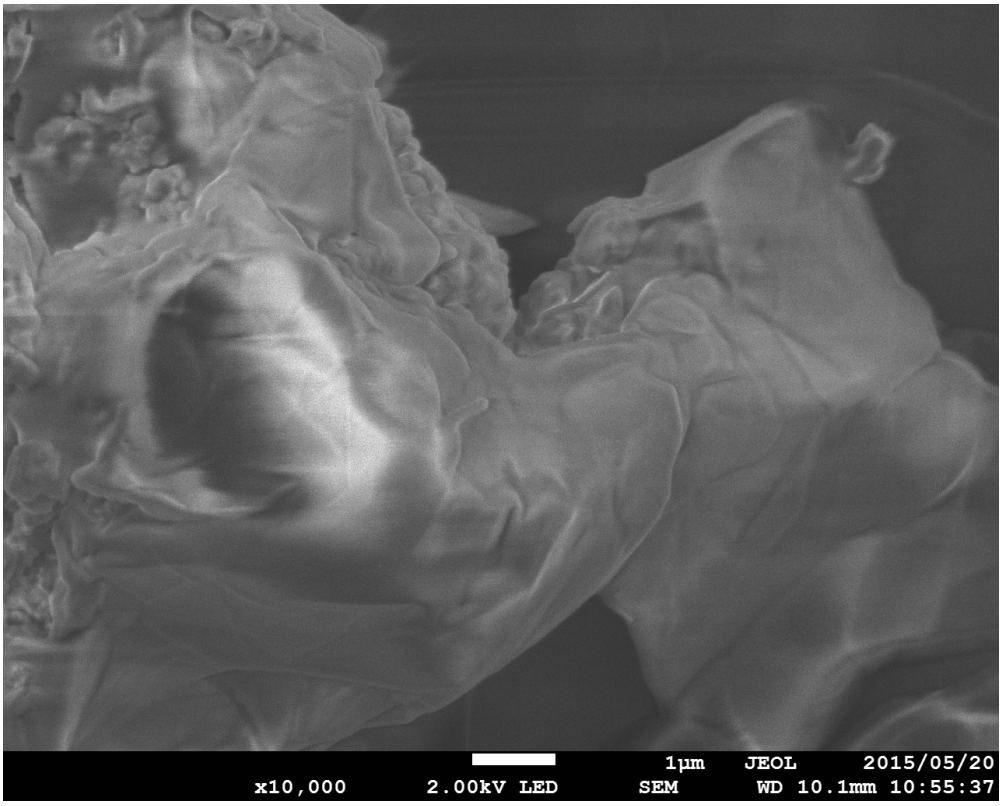
1µm JEOL 2015/05/20
x10,000 2.00kV LED SEM WD 10.1mm 10:55:37

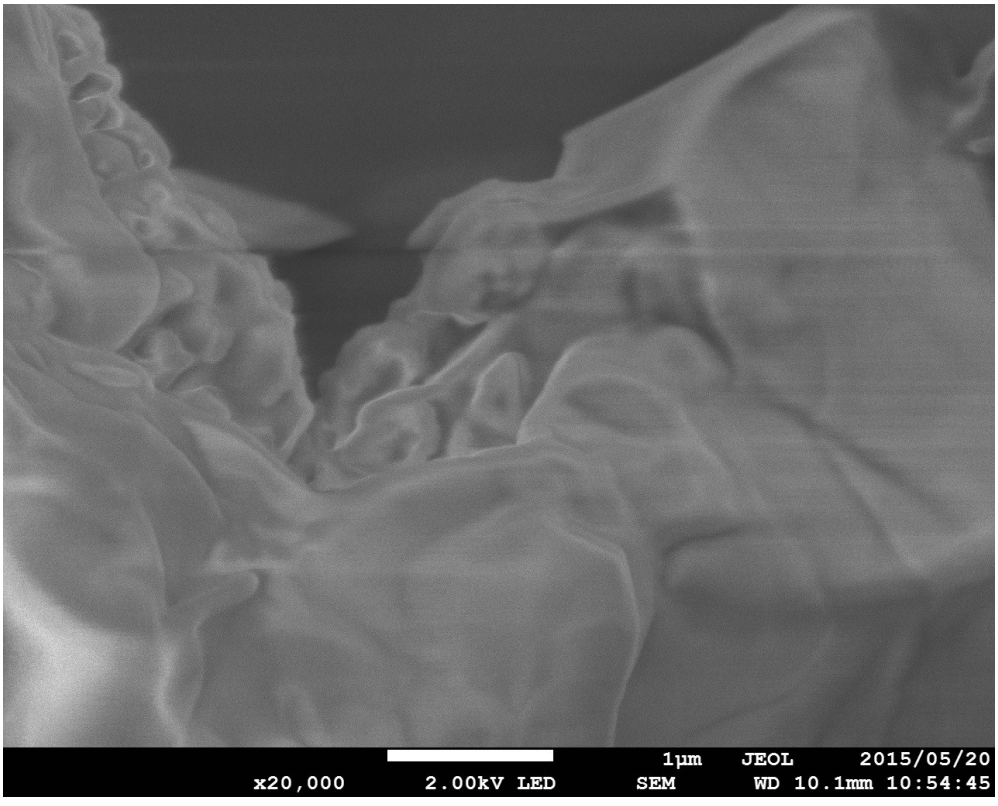
1µm JEOL 2015/05/20
x20,000 2.00kV LED SEM WD 10.1mm 10:54:45

(**d**)

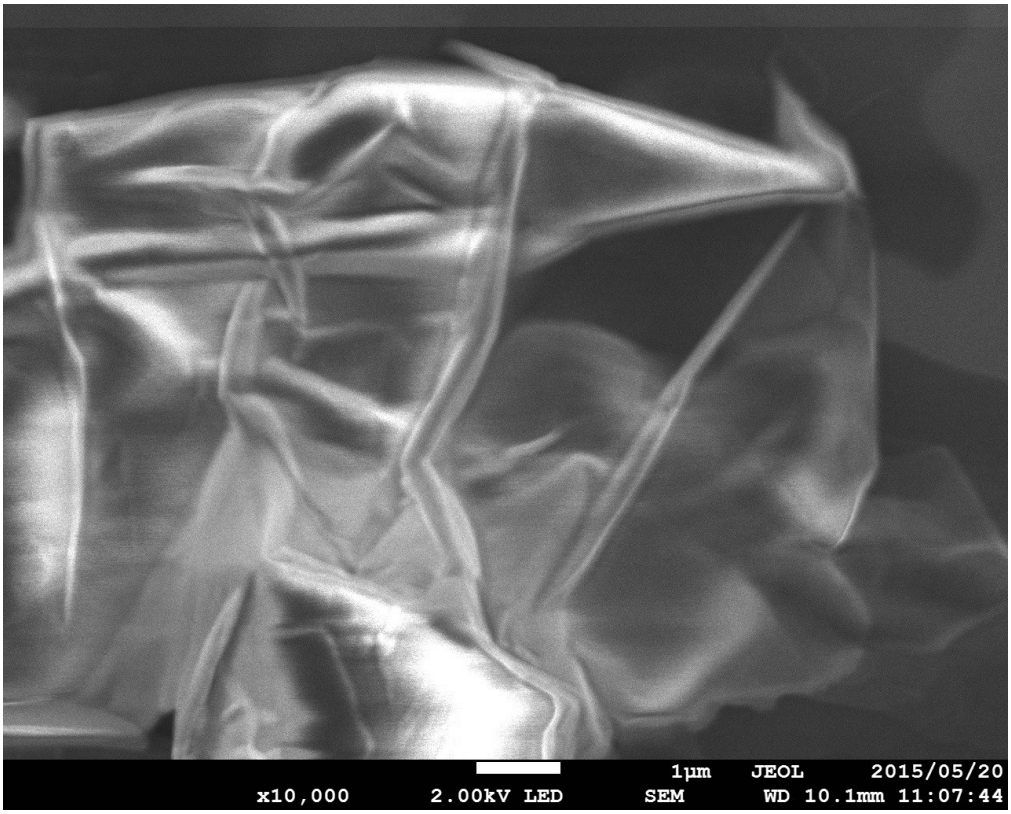

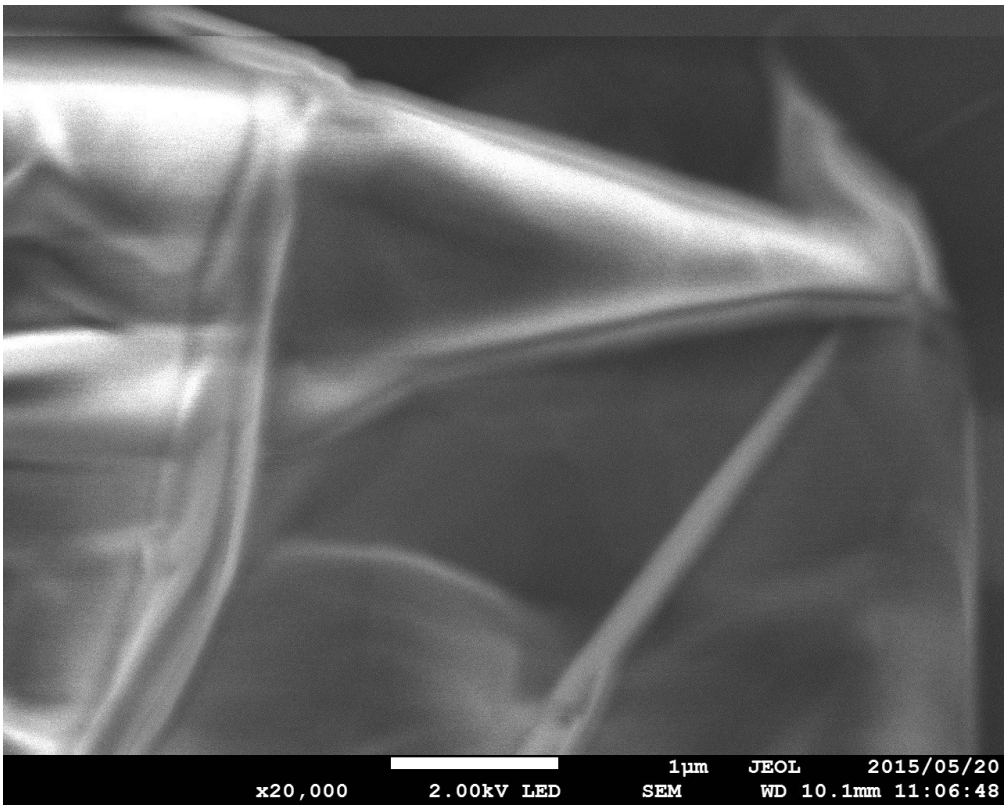

Fig. S2 SEM images of few-layered CP **2** via physical exfoliation (**a**); via in situ

synthesis in the presence of PVP, PVP/ligand = 1: 100 (**b**); PVP/ligand = 1: 200 (**c**); in the presence of PEG 6000, PEG/ligand = 1:60 (**d**).

(**a**)

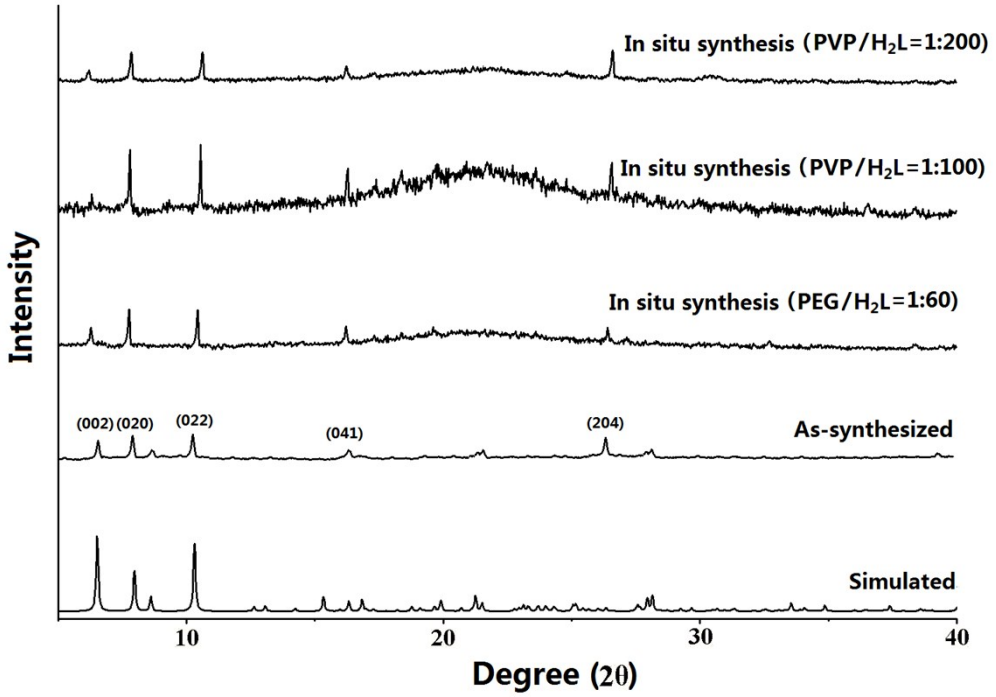

(**b**)

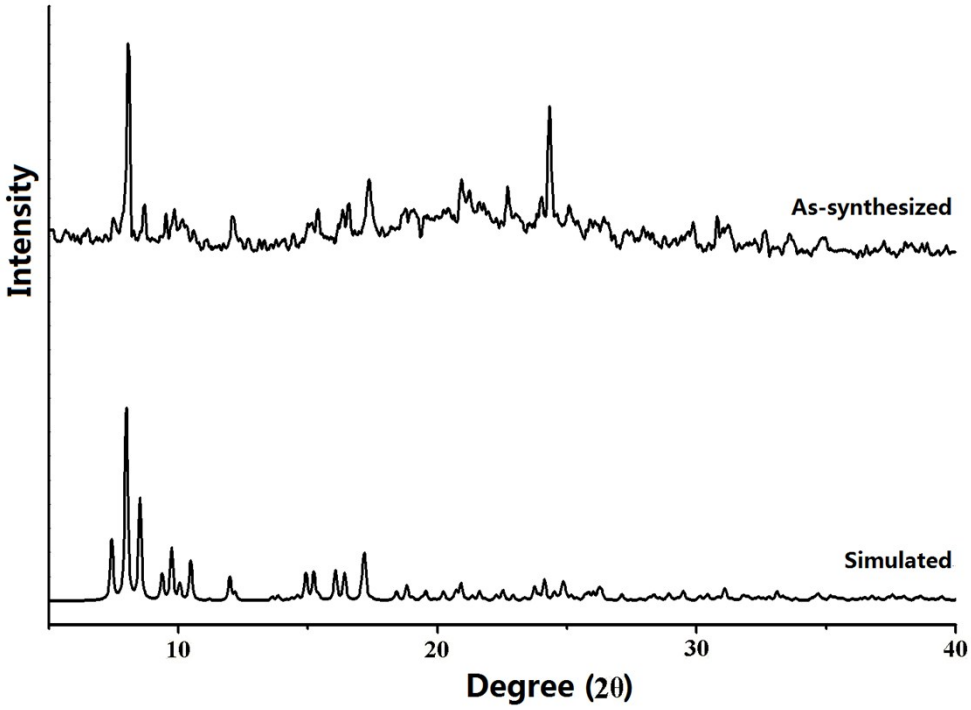

Fig. S3 The powder XRD patterns of CPs **1** (**a**) and **2 (b).**

(**a**)

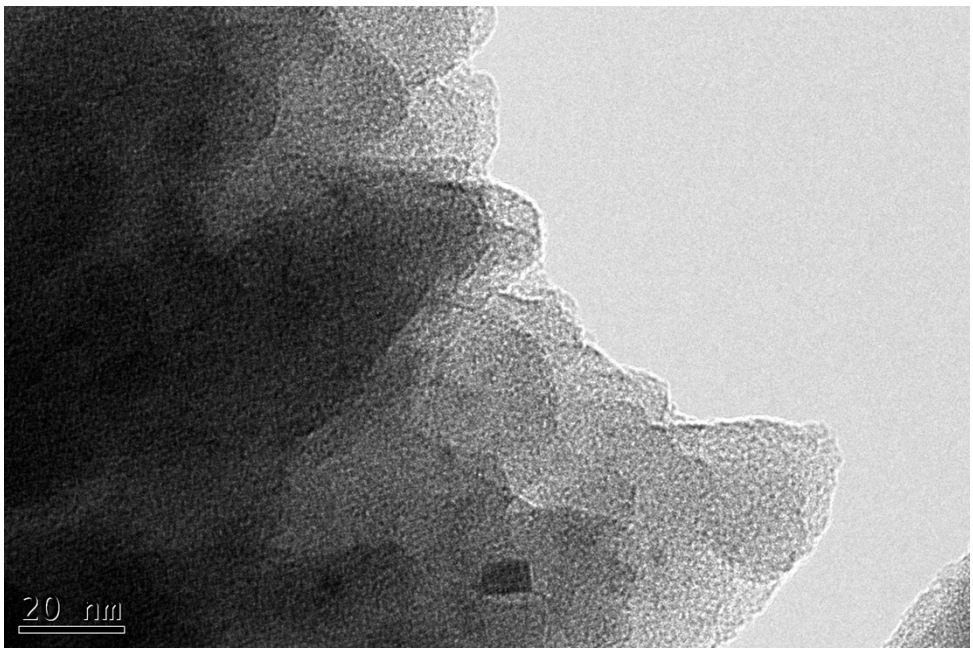

(**b**)

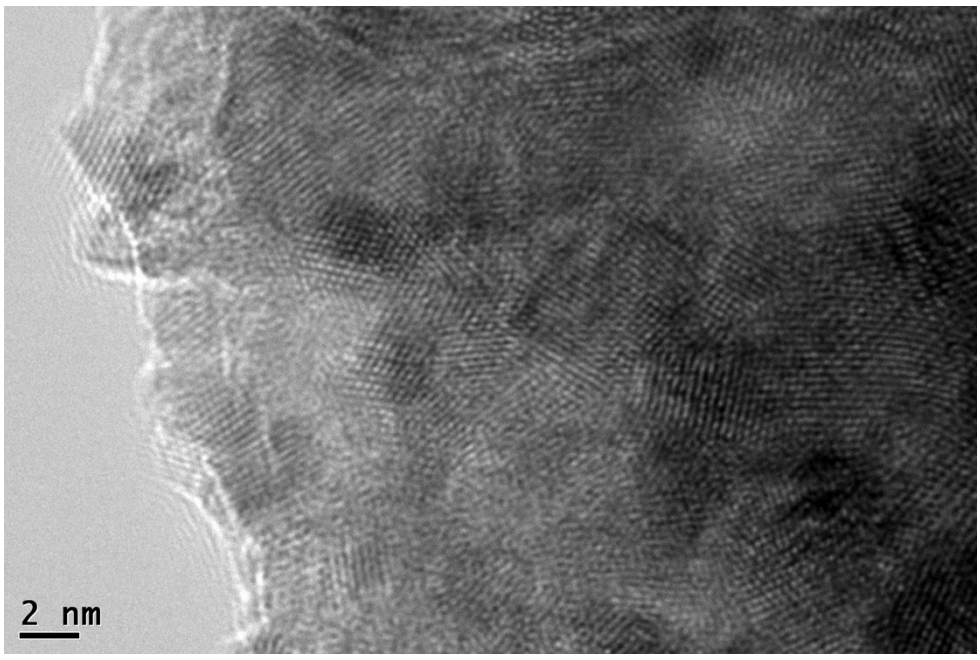

(**c**)

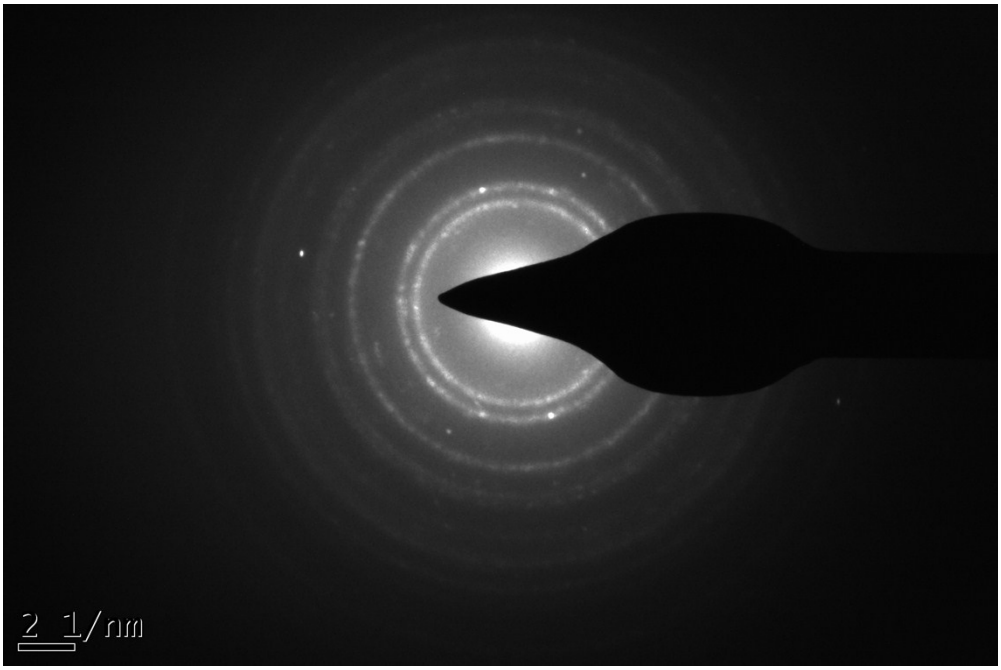

Fig. S4 Low- (**a**), high-magnification TEM images **(b**) and selected area electron diffraction (SAED) (**c**) of the few-layered CP **2.**

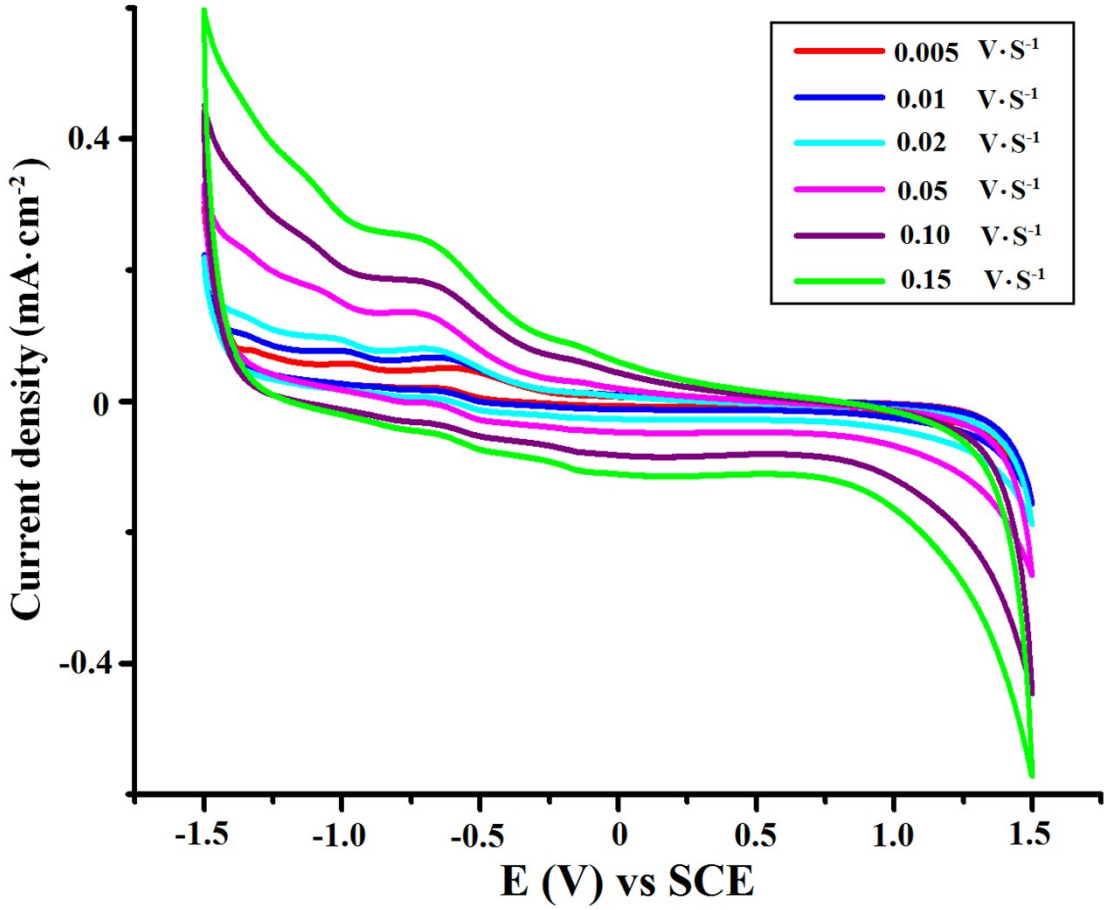

Fig. S5 CVs of the bare GCE in an aqueous solution buffered to neutral pH (pH = 6.8, H_3PO_4/NaOH, 0.05 M) at different sweep rates.

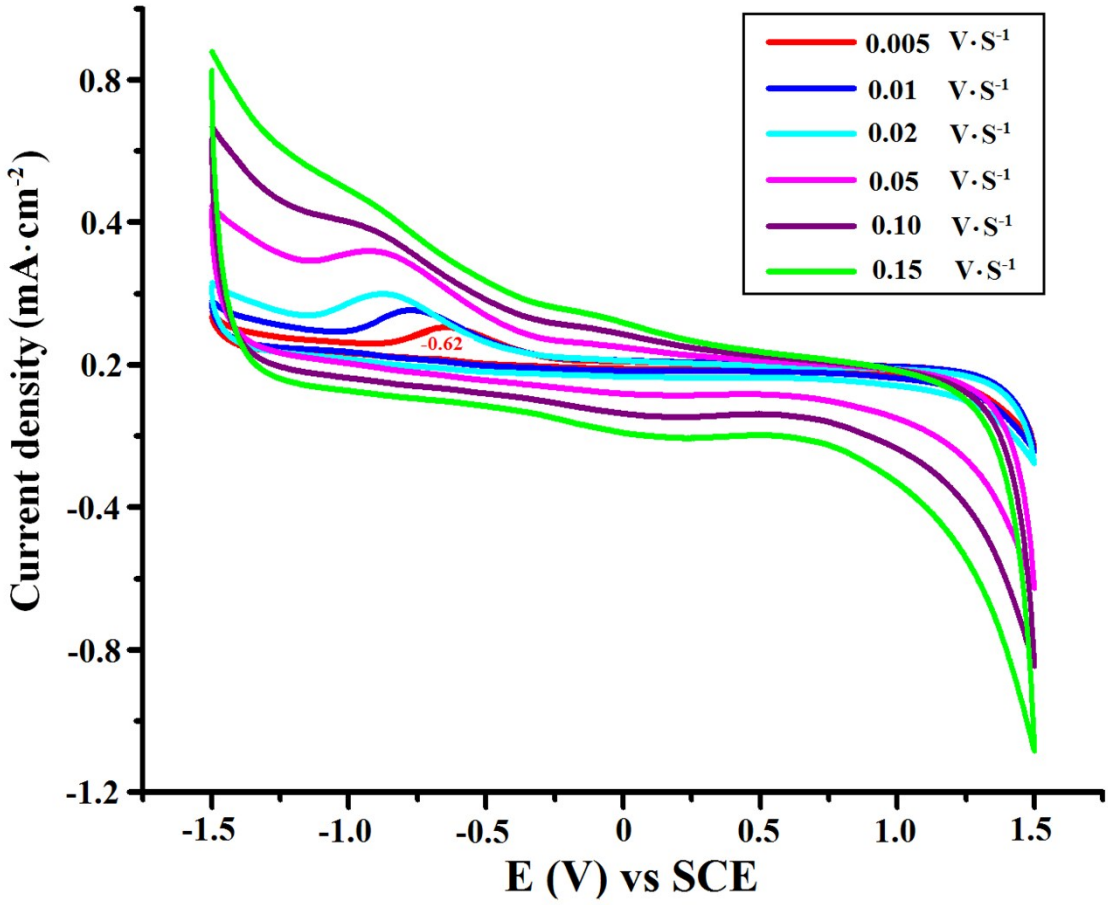

Fig. S6 CVs of **H_2L-GCE** in an aqueous solution buffered to neutral pH (pH = 6.8, H_3PO_4/NaOH, 0.05 M) at different sweep rates.

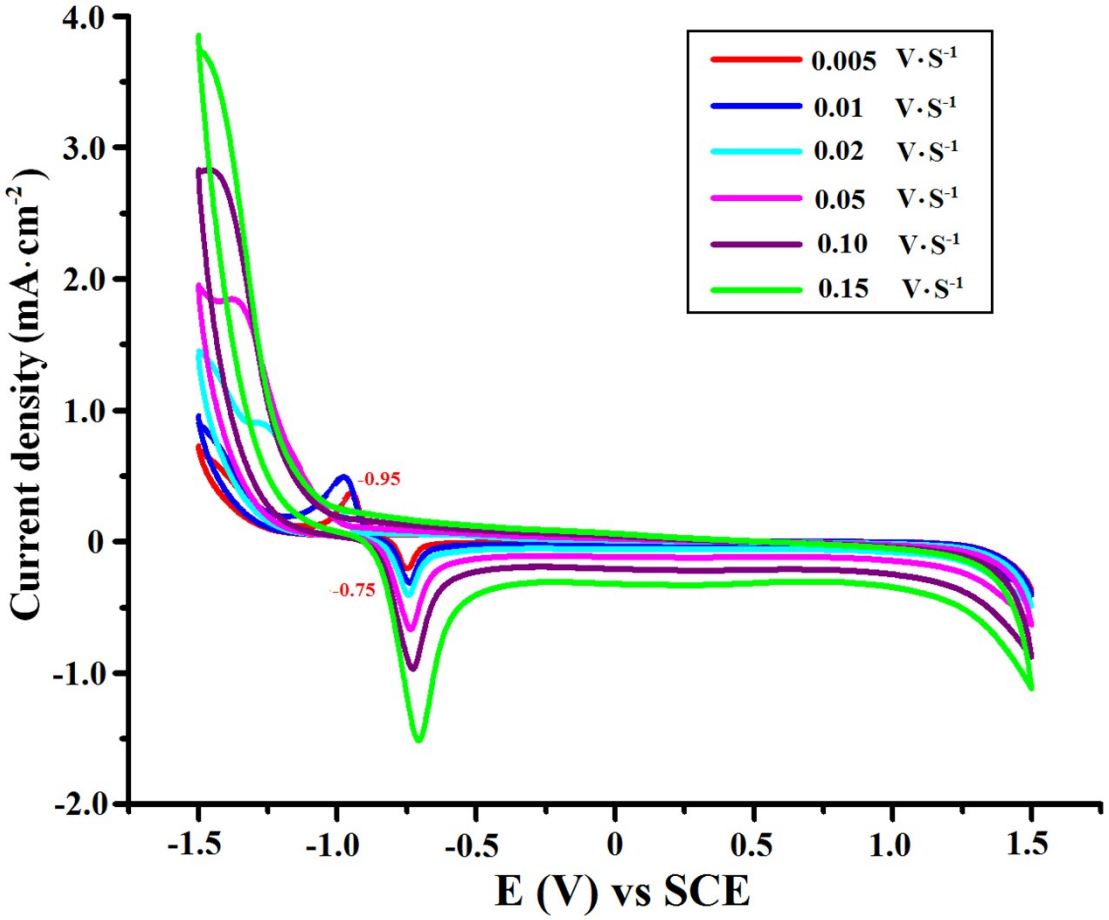

Fig. S7 CVs of **1-GCE** in an aqueous solution buffered to neutral pH (pH = 6.8, H_3PO_4/NaOH, 0.05 M) at different sweep rates.

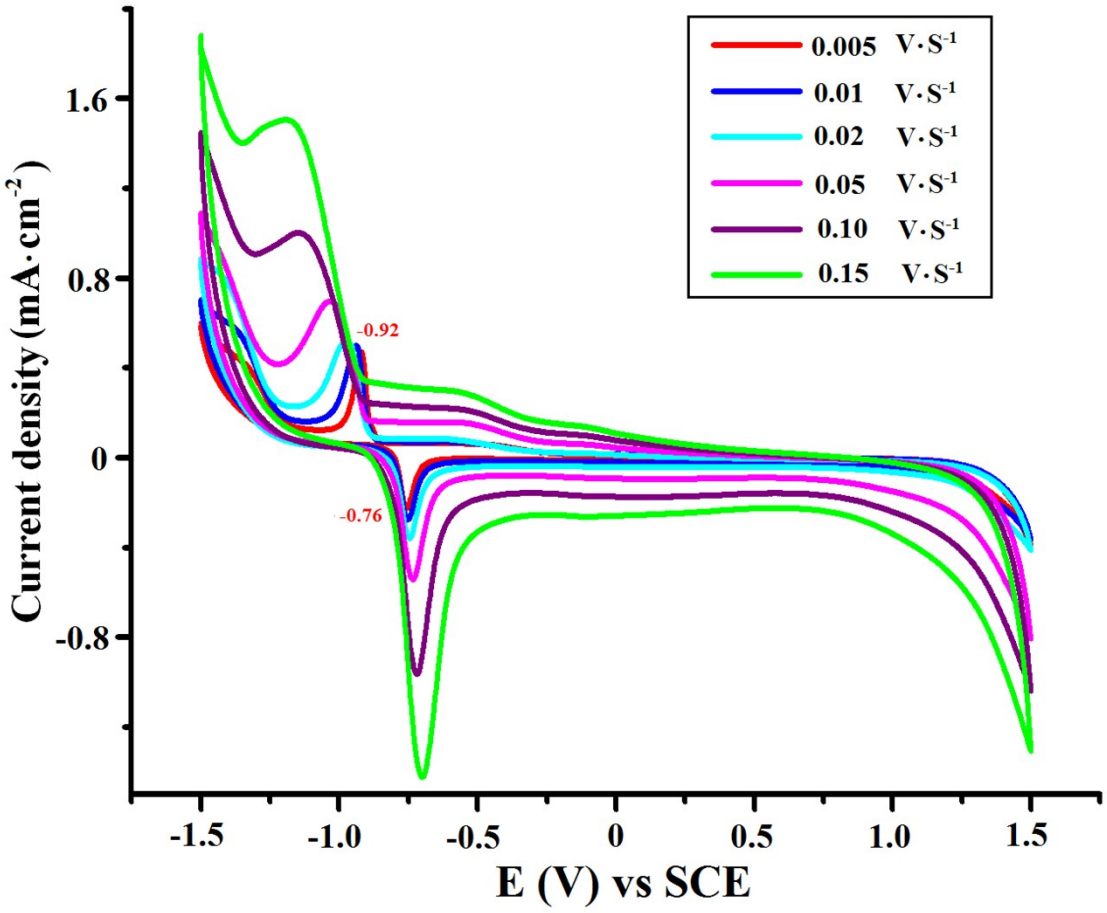

Fig. S8 CVs of **2-GCE** in an aqueous solution buffered to neutral pH (pH = 6.8, H_3PO_4/NaOH, 0.05 M) at different sweep rates.

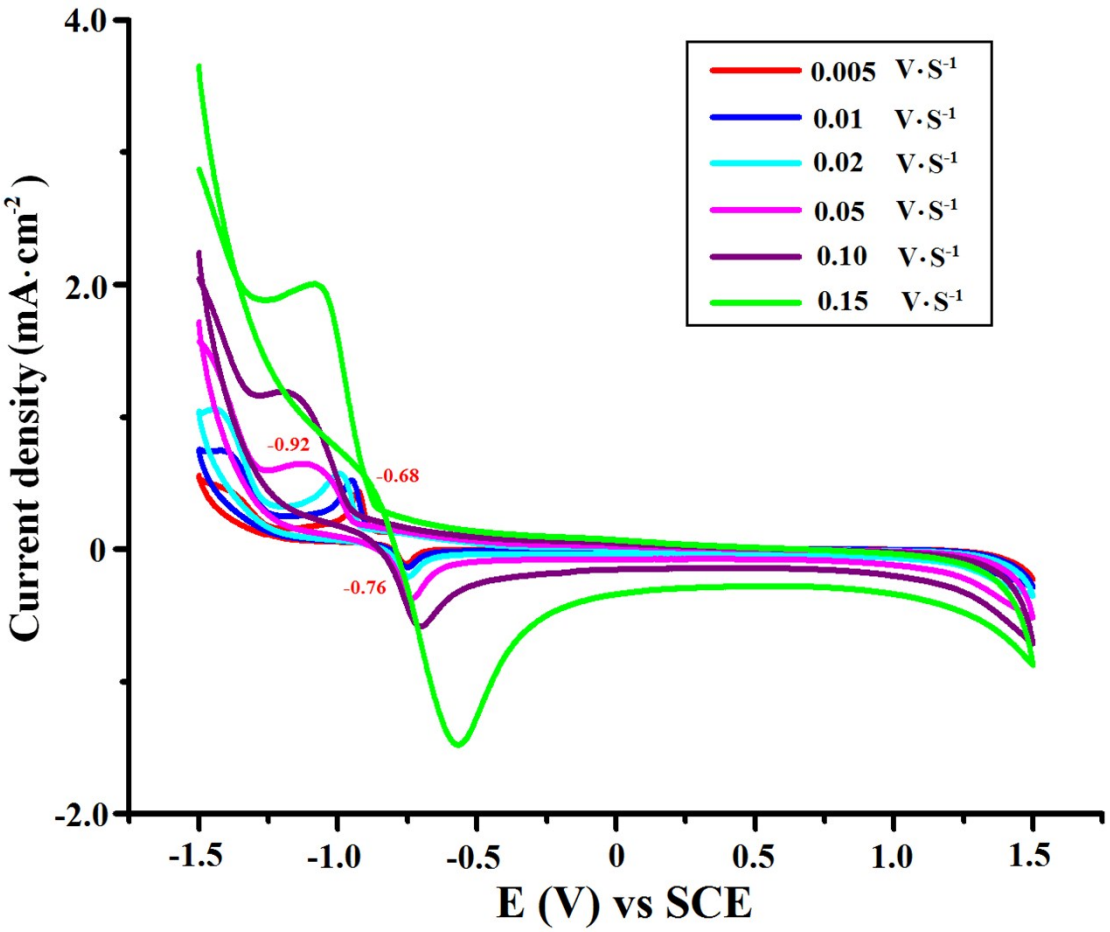

Fig. S9 CVs of the few-layered CP **2**-modified GCE in an aqueous solution buffered to neutral pH (pH = 6.8, H_3PO_4/NaOH, 0.05 M) at different sweep rates.

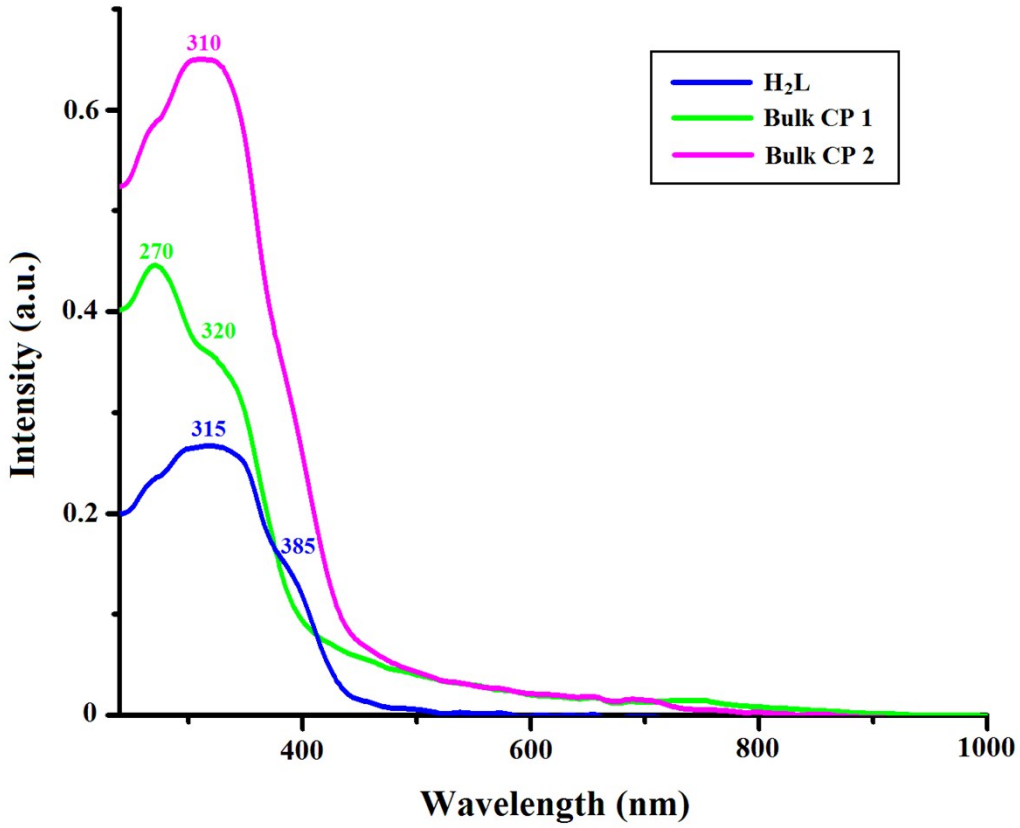

Fig. S10 UV-vis absorption spectra for bulk CPs **1-2** and **H_2L** in the solid state.

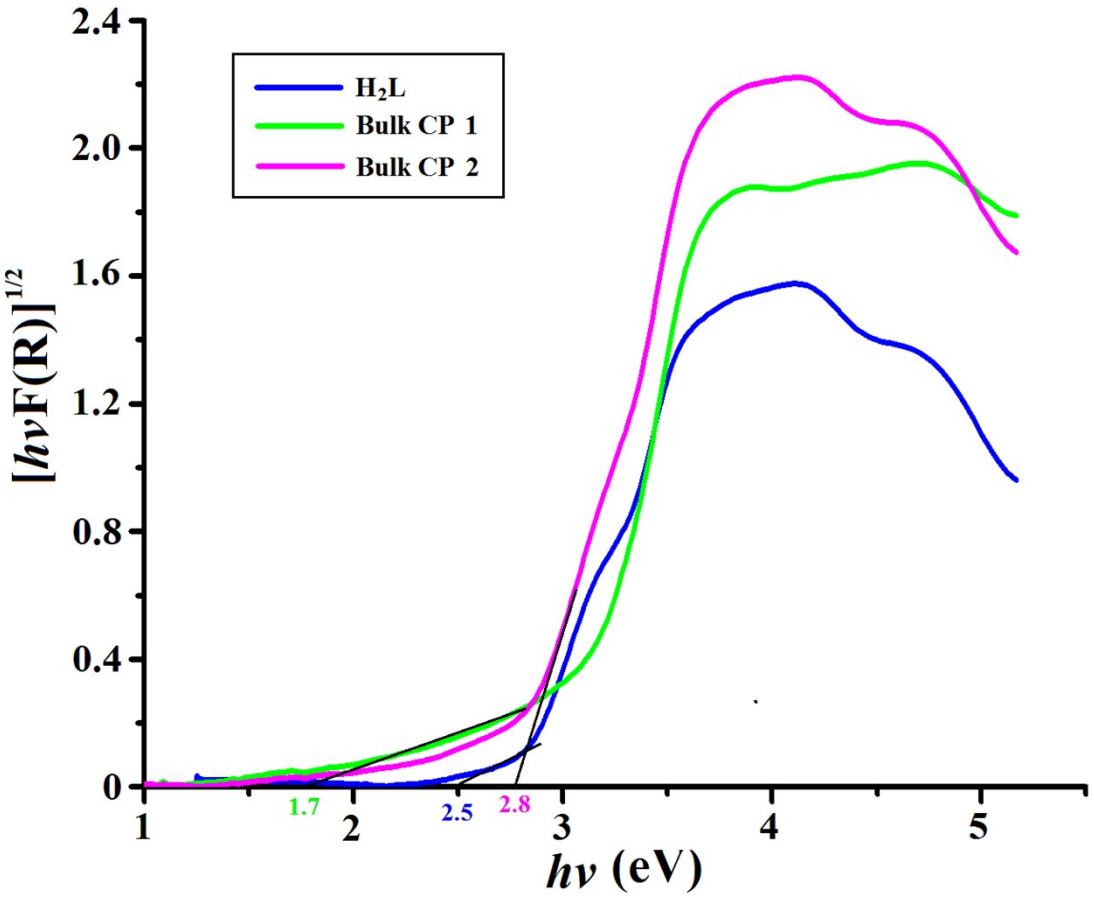

Fig. S11 The diffuse reflectance spectra of **H_2L,** bulk CPs **1** and **2** in Kubelka–Munk functions.

The diffuse reflectance spectra of **H_2L** and CPs **1-2** are shown in **Fig. S11**. The correlation between the absorption coefficient of allowed indirect semiconductor and optical band gap E_{gap} can be determined by the equation

$$\alpha E \approx A_1(E-E_{gap})^2 \qquad (1)$$

where $E = h\nu$ is the photon energy, A_1 is a constant.

F(R) is the Kubelka−Munk equation, which is expressed as

$$F(R) = (1-R)^2/2R = k/s \qquad (2)$$

where R is the experimentally observed reflectance of the sample, k is the molar absorption coefficient, and s is the scattering coefficient. The scattering coefficients are weakly dependent on the wavelength of the incident light, and using eqs 1 and 2, the following eq 3 can be obtained:

$$[h\nu F(R)]^{1/2} = A_2[h\nu - E_{gap}] \qquad (3)$$

From the plot of $[h\nu F(R)]^{1/2}$ versus $h\nu$, by extrapolating the linear fitted regions to $[h\nu F(R)]^{1/2}=0$, the value of optical band gaps E_{gap} of $\mathbf{H_2L}$ and CPs **1-2** are ca. 2.5, 1.7 and 2.8 eV, respectively.

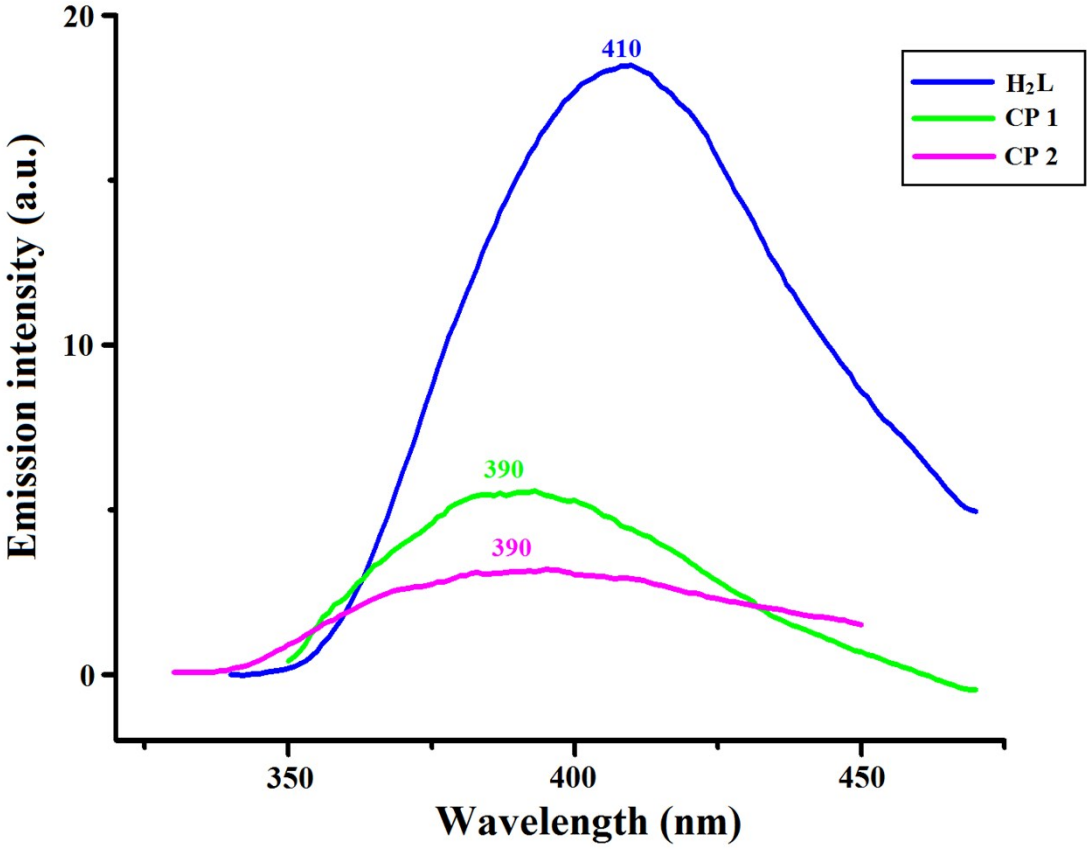

Fig. S12 Solid-state emission spectra at room temperature for $\mathbf{H_2L}$ and CPs **1-2** (slit width = 10 nm).

(a)

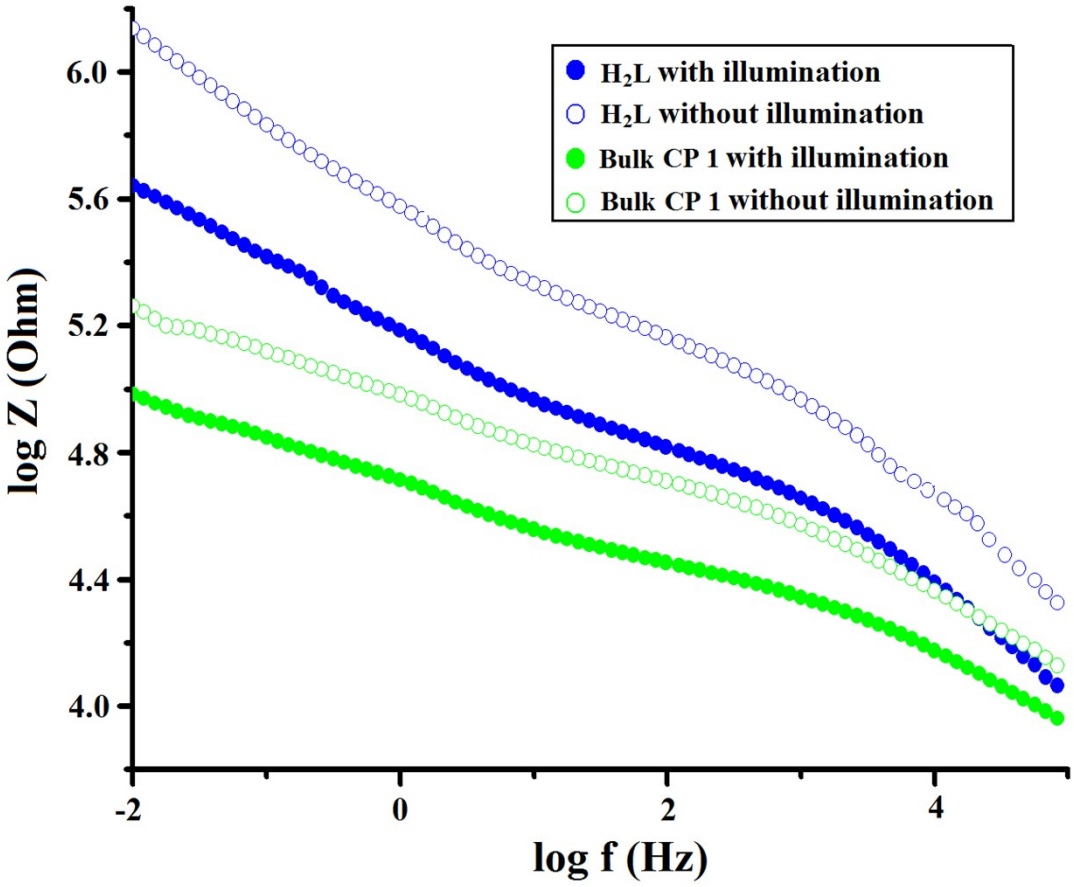
H2L with illumination
H2L without illumination
Bulk CP 1 with illumination
Bulk CP 1 without illumination
log Z (Ohm)
6.0
5.6
5.2
4.8
4.4
4.0
-2
0
2
4
log f (Hz)

(b)

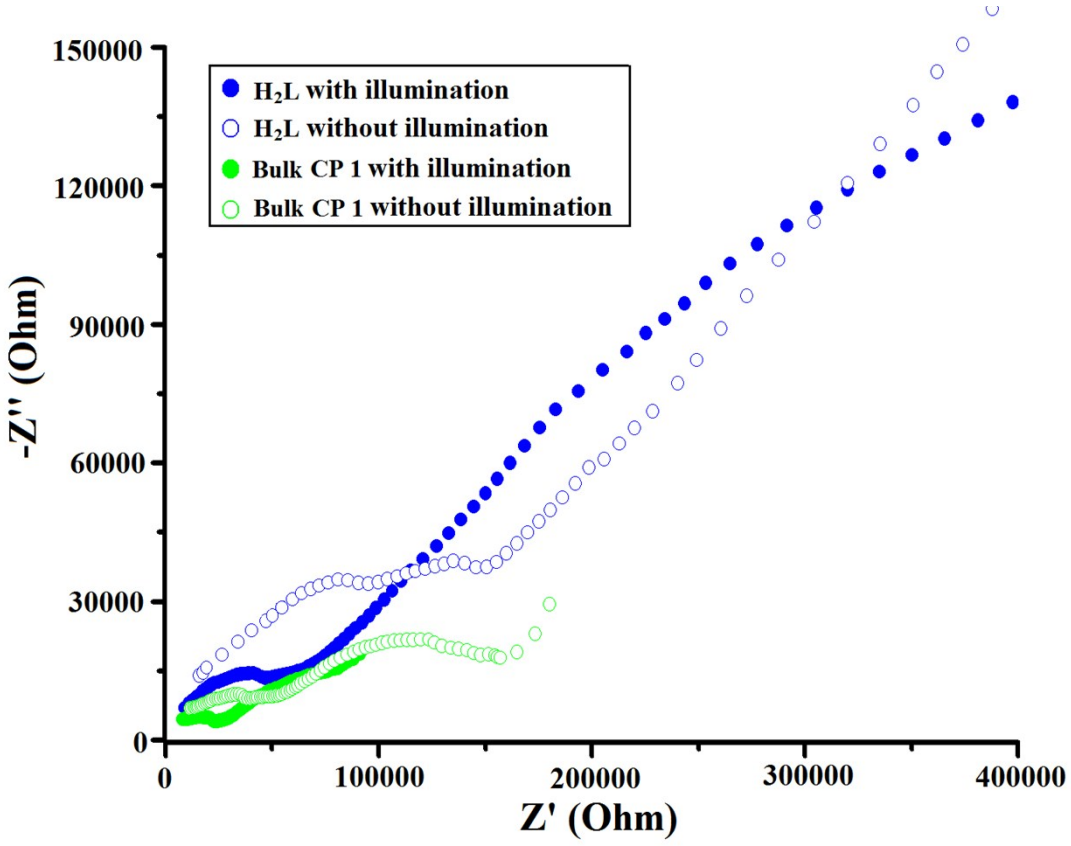

Fig. S13 Bode plots (log of impedance magnitude vs. log f) (**a**) and Nyquist plots (Z' vs. $-Z''$) (**b**) of the three-electrode systems at E = 0 V vs Ag/AgCl in aqueous phosphate solution (0.05 M, pH = 6.8) in the absence and presence of visible light illumination ($\lambda >$ 400 nm) with **1-FTO** and **H_2L-FTO** as working electrodes, respectively.

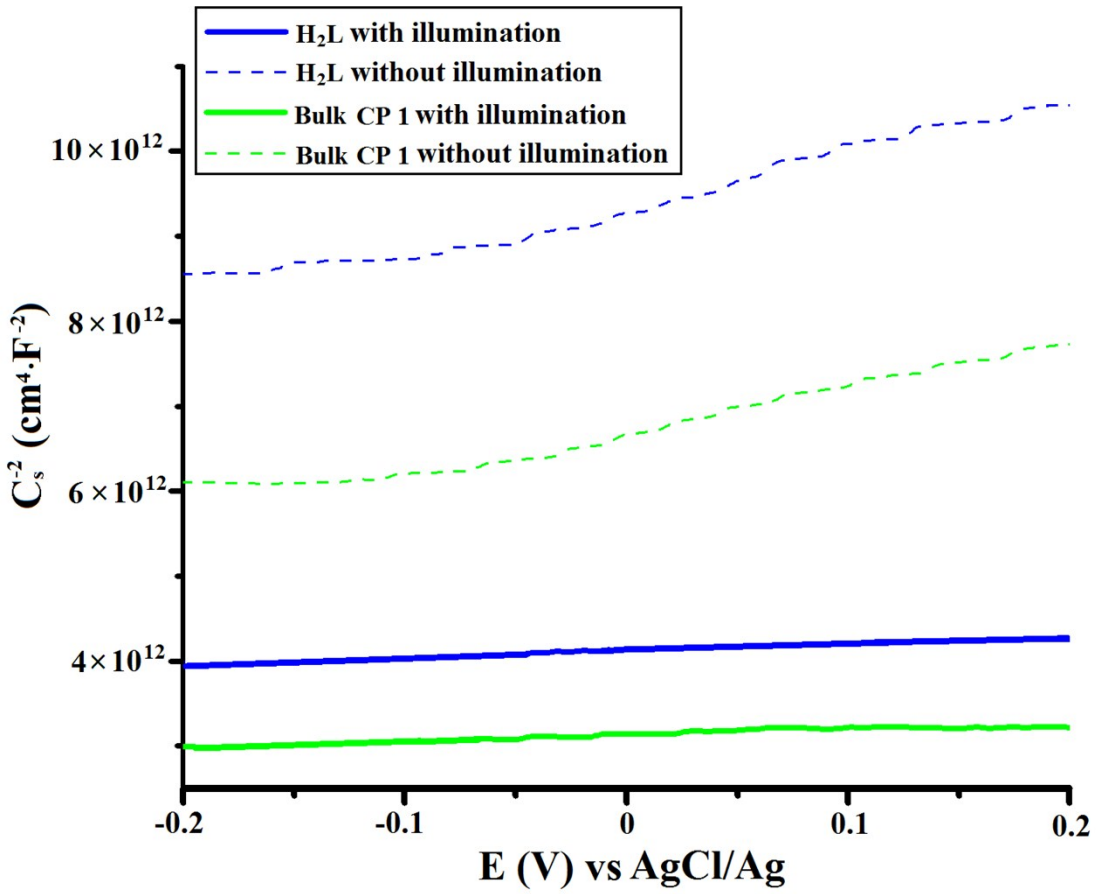

Fig. S14 Mott–Schottky curves of **H_2L-FTO** and **1-FTO** (ac amplitude: 5 mV, frequency: 1000 Hz) in the absence and presence of visible light illumination ($\lambda > 400$ nm).

(**a**)

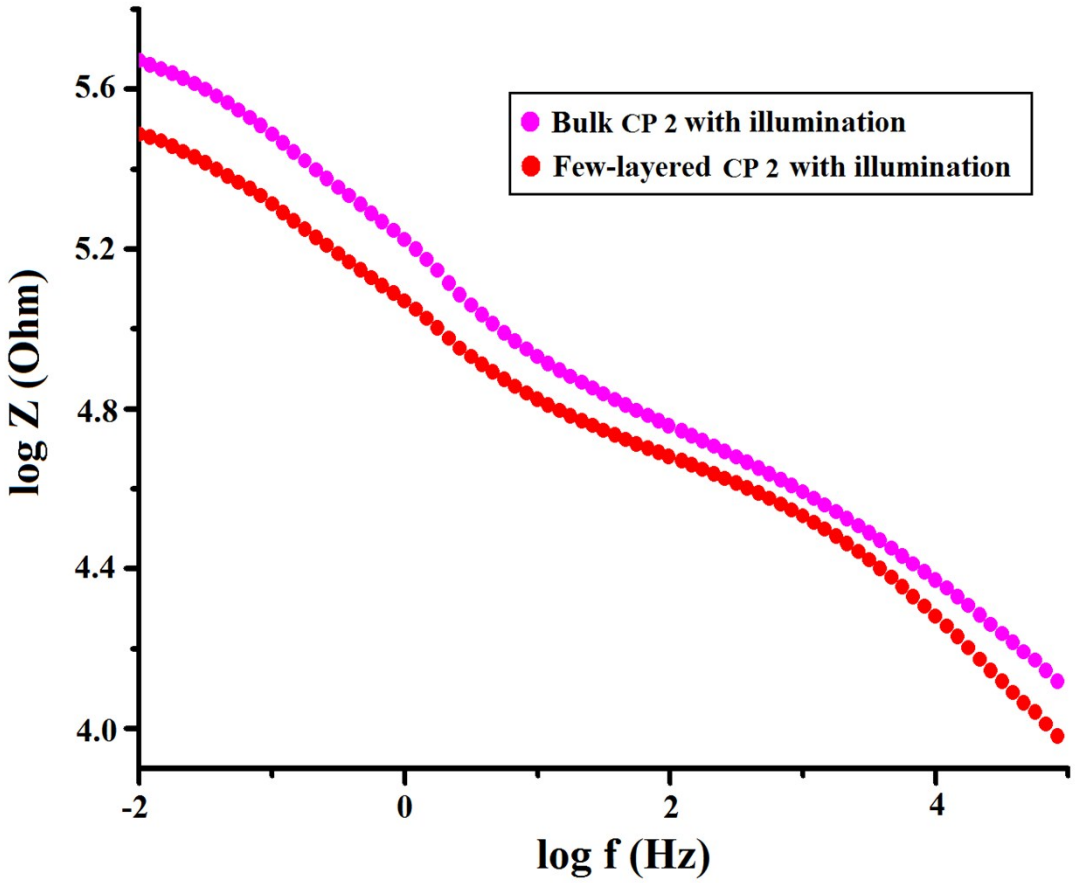
Bulk CP 2 with illumination
Few-layered CP 2 with illumination
log Z (Ohm)
5.6
5.2
4.8
4.4
4.0
-2
0
2
4
log f (Hz)

(**b**)

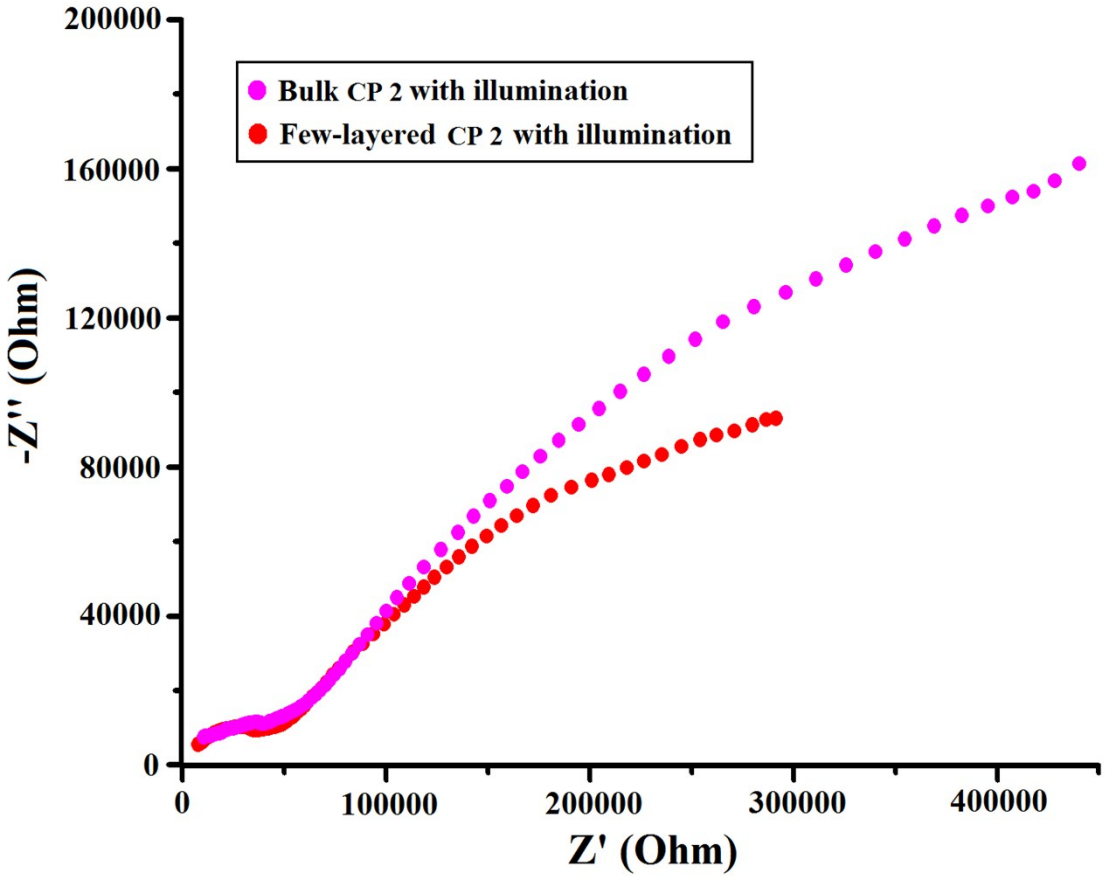

Fig. S15 Bode plots (log of impedance magnitude vs. log f) (**a**) and Nyquist plots (Z' vs. $-Z''$) (**b**) of the three-electrode systems at E = 0 V vs Ag/AgCl in aqueous phosphate solution (0.05 M, pH = 6.8) in the presence of visible light illumination (λ > 400 nm) with **2-FTO** and the few-layered CP **2**-modified **FTO** as working electrodes, respectively.

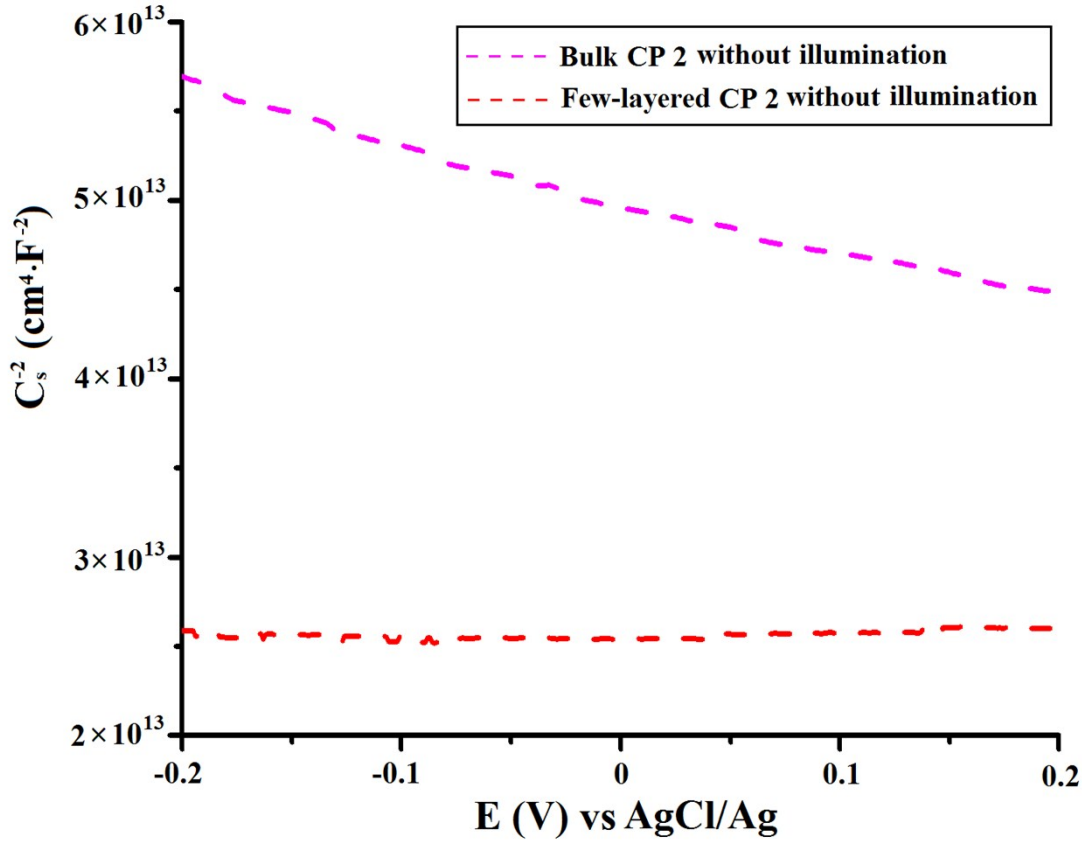

Fig. S16 Mott–Schottky curves of **2-FTO** and the few-layered CP **2**-modified **FTO** (ac amplitude: 5 mV, frequency: 1000 Hz) in the absence of visible light illumination.

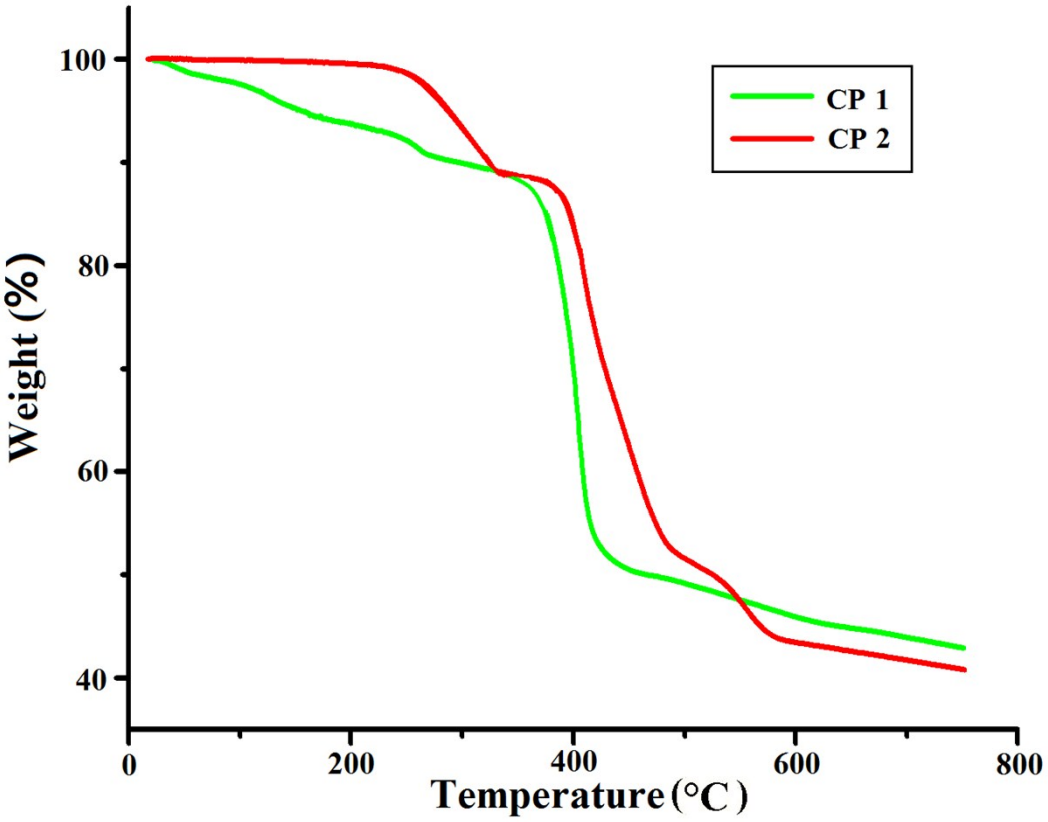

Fig. S17 Thermogravimetric curves of CPs **1** and **2**.